Article

Invasive and Adherent Bacterial Pathogens Co-Opt Host Clathrin for Infection

Esteban Veiga,[1,2,3,8,*] Julian A. Guttman,[4,8,10] Matteo Bonazzi,[1,2,3,9] Emmanuel Boucrot,[5,9]
Alejandro Toledo-Arana,[1,2,3,9] Ann E. Lin,[4] Jost Enninga,[6,7] Javier Pizarro-Cerdá,[1,2,3] B. Brett Finlay,[4]
Tomas Kirchhausen,[5] and Pascale Cossart[1,2,3,*]
[1]Institut Pasteur, Unité des Interactions Bactéries-Cellules, Paris F-75015, France
[2]INSERM, U604, Paris F-75015, France
[3]INRA, USC2020, Paris F-75015, France
[4]The University of British Columbia, Michael Smith Laboratories, 301-2185 East Mall, Vancouver, B.C. V6T 1Z4 Canada
[5]Department of Cell Biology and Immune Disease Institute, Harvard Medical School, 200 Longwood Avenue, Boston,
MA 02115, USA
[6]Unite de Pathogenie Microbienne Moleculaire, Institut Pasteur 25, Rue du Dr. Roux, Paris F-75015, France
[7]INSERM U786, Paris F-75015, France
[8]These authors contributed equally to this work.
[9]These authors contributed equally to this work.
[10]Present address: Department of Biological Sciences, Shrum Science Centre, Simon Fraser University, 8888 University Drive,
Room B8276, Burnaby, British Columbia V5A 1S6, Canada.
*Correspondence: eveiga@pasteur.fr (E.V.), pcossart@pasteur.fr (P.C.)
DOI 10.1016/j.chom.2007.10.001

SUMMARY

Infection by the bacterium *Listeria monocyto-genes* depends on host cell clathrin. To determine whether this requirement is widespread, we analyzed infection models using diverse bacteria. We demonstrated that bacteria that enter cells following binding to cellular receptors (termed "zippering" bacteria) invade in a clathrin-dependent manner. In contrast, bacteria that inject effector proteins into host cells in order to gain entry (termed "triggering" bacteria) invade in a clathrin-independent manner. Strikingly, enteropathogenic *Escherichia coli* (EPEC) required clathrin to form actin-rich pedestals in host cells beneath adhering bacteria, even though this pathogen remains extracellular. Furthermore, clathrin accumulation preceded the actin rearrangements necessary for *Listeria* entry. These data provide evidence for a clathrin-based entry pathway allowing internalization of large objects (bacteria and ligand-coated beads) and used by "zippering" bacteria as part of a general mechanism to invade host mammalian cells. We also revealed a nonendocytic role for clathrin required for extracellular EPEC infections.

INTRODUCTION

Clathrin-mediated endocytosis is the main process by which many transmembrane proteins are internalized from the plasma membrane (Conner and Schmid, 2003; Kirchhausen, 2000; McNiven and Thompson, 2006).

These transmembrane proteins recruit intracellular adaptor proteins that, together with clathrin, form an endocytic coated pit at the plasma membrane that continuously invaginates, finally pinching off the membrane to form a clathrin-coated vesicle. Clathrin surrounding the newly formed endocytic vesicle is rapidly disassembled (Kirchhausen, 2000; Massol et al., 2006; Sorkin, 2004). The size of coated vesicles varies from 30 to 150 nm (Cheng et al., 2007; Ehrlich et al., 2004; McMahon, 1999), indicating an upper limit of ~150 nm in the size of the engulfed objects. However, the invasion of some viruses (e.g., parvovirus, influenza, or reovirus), which are well known to enter host cells by clathrin-dependent endocytosis (Ehrlich et al., 2004; Marsh and Helenius, 2006), has been reported to occur through vesicles larger that 150 nm (Matlin et al., 1981; Parker and Parrish, 2000). Significantly, large clathrin assemblies have also been observed by electron microscopy in endosomes (Raiborg et al., 2006), in the plasma membrane (Heuser, 1989), and surrounding opsonized beads (Aggeler and Werb, 1982).

Invasive bacteria induce their own uptake by nonphagocytic host cells using two well-differentiated mechanisms referred to as "zippering" and "triggering" (Cossart and Sansonetti, 2004; Veiga and Cossart, 2006). Zippering bacteria such as *Listeria monocytogenes*, *Yersinia pseudotuberculosis*, and *Staphyloccocus aureus* express invasion proteins on their surface that interact directly or indirectly with cellular receptors, initiating signaling cascades that result in actin polymerization and membrane extensions that zip around and engulf entering bacteria (Pizarro-Cerda and Cossart, 2006a). *Listeria* invasion proteins InlA and InlB interact with cellular E-cadherin and Met, respectively (Gaillard et al., 1991; Lecuit et al., 1999; Shen et al., 2000); *Yersinia* invasin (inv) directly binds to β1-integrin (Isberg and Leong, 1990), while *Staphyloccocus* express fibronectin-binding proteins allowing bacterial entry by indirect engagement of β1-integrin through

the interaction of the latter with fibronectin (Agerer et al., 2005; Grundmeier et al., 2004). *Salmonella typhimurium* and *Shigella flexneri* are paradigms of bacteria that use the trigger mechanism (Cossart and Sansonetti, 2004). These bacteria use a specialized secretory apparatus, the type III secretion system (T3SS), to inject bacterial effector proteins into the host cytoplasm to modulate the host actin cytoskeleton, triggering massive polymerization of actin and membrane ruffling, resulting in bacterial internalization in a process similar to macropinocytosis (Cossart and Sansonetti, 2004; Pizarro-Cerda and Cossart, 2006a). Enteropathogenic *Escherichia coli* (EPEC), which remain extracellular, also use a T3SS to hijack the actin cytoskeleton of the host cell including N-WASP and Arp2/3 and form an actin-rich pedestal beneath the adherent organisms (Goosney et al., 2000).

It was generally assumed that bacteria enter into host cells by mechanisms independent of clathrin-mediated endocytosis. Nevertheless, we recently showed that *L. monocytogenes* uses the InlB/Met pathway to enter host cells through a clathrin-dependent mechanism (Veiga and Cossart, 2005). In the present study, we investigated whether the clathrin-dependent *Listeria* entry is an exception or whether clathrin is a common target during bacterial pathogenesis.

RESULTS

Zippering Bacteria Recruit Clathrin and Dynamin during Invasion

To address whether bacteria exploit a clathrin-dependent mechanism to invade nonphagocytic cells, we examined *Y. pseudotuberculosis*, *S. aureus*, and *L. monocytogenes* as models of zippering bacteria. To focus our analysis to the invasin-integrin pathway, we used a noninvasive *E. coli* strain expressing the *Y. pseudotuberculosis* invasin (inv), *E. coli* (inv), which mimics the entry of *Yersinia* (Isberg and Falkow, 1985). In the case of *Listeria*, to study exclusively the InlA pathway, we used a nonpathogenic and noninvasive strain, *Listeria innocua*, harboring a plasmid allowing the expression of InlA, *L. innocua* (inlA). This strain has been typically used to study *Listeria* internalization via the InlA-E-cadherin pathway (Gaillard et al., 1991; Lecuit et al., 1999).

Adherent human epithelial cells were infected with one of the three bacteria: *E. coli* (inv), *S. aureus*, or *L. innocua* (inlA). For *E. coli* (inv) and *S. aureus* infection, we used HeLa cells, but, as HeLa do not express E-cadherin (and therefore *Listeria* cannot enter via InlA), *Listeria* infections were performed in JEG3 cells. As shown in Figures 1A–1C, using a monoclonal antibody to visualize the clathrin heavy chain, clathrin colocalized with entering bacteria. The presence of clathrin was also observed in BSC1 cells in the case of *E. coli* (inv) and *S. aureus* infections and in Caco-2 cells during *L. innocua* (inlA) infections (data not shown).

Maturation of clathrin-coated pits normally occurs through the recruitment of a large collection of clathrin-associated proteins including the GTPase dynamin (Conner and Schmid, 2003; Kirchhausen, 2000), which is required for subsequent vesicle scission (Ehrlich et al., 2004; Hinshaw, 2000; Macia et al., 2006; Merrifield et al., 2005; Orth and McNiven, 2003). We therefore followed the localization of dynamin during bacterial infection in the same conditions as described above. Dynamin colocalized with *E. coli* (inv), *S. aureus* and *L. innocua* (inlA) during entry (see Figure S1 in the Supplemental Data available with this article online). The presence of clathrin and dynamin, hallmark proteins of clathrin-dependent endocytosis, at the bacterial entry site suggested a possible role for receptor-mediated endocytosis in bacterial entry.

A Functional Clathrin-Dependent Internalization Machinery Is Necessary for Bacterial Entry

To further examine whether bacterial entry involves elements of the typical clathrin-dependent endocytic machinery, we analyzed bacterial entry into cells in which expression of clathrin and dynamin was knocked-down (KD) by siRNA. Cells in which clathrin expression was altered were infected with *E. coli* (inv), *S. aureus*, or *L. innocua* (inlA) for 1 hour, and extracellular bacteria were then killed by adding gentamicin. Intracellular, invasive bacteria were counted by cell lysate plating. As shown in Figure 2A, a 5-fold decrease for *E. coli* (inv) and *S. aureus* invasion was detected in clathrin-KD cells. A similar decrease in entry was detected in dynamin-KD cells challenged with *E. coli* (inv), while a more dramatic effect was detected in the entry of *S. aureus* (Figures 2A and 2B). The entry of *L. innocua* (inlA) was inhibited more than 2-fold in clathrin or dynamin-KD cells.

To corroborate the role of dynamin in the entry of these bacteria, we determined their invasion rate in the presence or absence of dynasore, a cell-permeable specific inhibitor of dynamin (Macia et al., 2006). We first demonstrated that dynasore had no toxic effect on the bacteria and did not inhibit bacterial multiplication (data not shown). We then confirmed that dynasore inhibits the endocytosis of transferrin, the prototypical ligand used to study clathrin-dependent endocytosis. Dynasore impeded the efficient endocytosis of fluorescent transferrin, which remained mainly at the plasma membrane. As expected, transferrin accumulated in endosomes in cells not exposed to dynasore (Figure 2C). In agreement with the dynamin-KD siRNA experiments, the presence of dynasore strongly inhibited the internalization of *E. coli* (inv), *S. aureus*, and *L. innocua* (inlA), (Figure 2D) as tested by gentamicin survival assays.

We also tested the role of Cbl and Grb2 in bacterial entry. Cbl (for Casitas B-lineage lymphoma) is an E3 ubiquitin ligase and multifunctional adaptor protein that is implicated in the regulation of signal transduction, internalization, and degradation of different membrane receptors including EGF (epidermal growth factor receptor) and Met (Dikic et al., 2003; Huang and Sorkin, 2005; Petrelli et al., 2002; Stang et al., 2004). It has also been shown that Cbl promotes the ubiquitination of integrins, their endocytosis, and, hence, the detachment of osteoclasts from fibronectin (Kaabeche et al., 2005). Growth factor
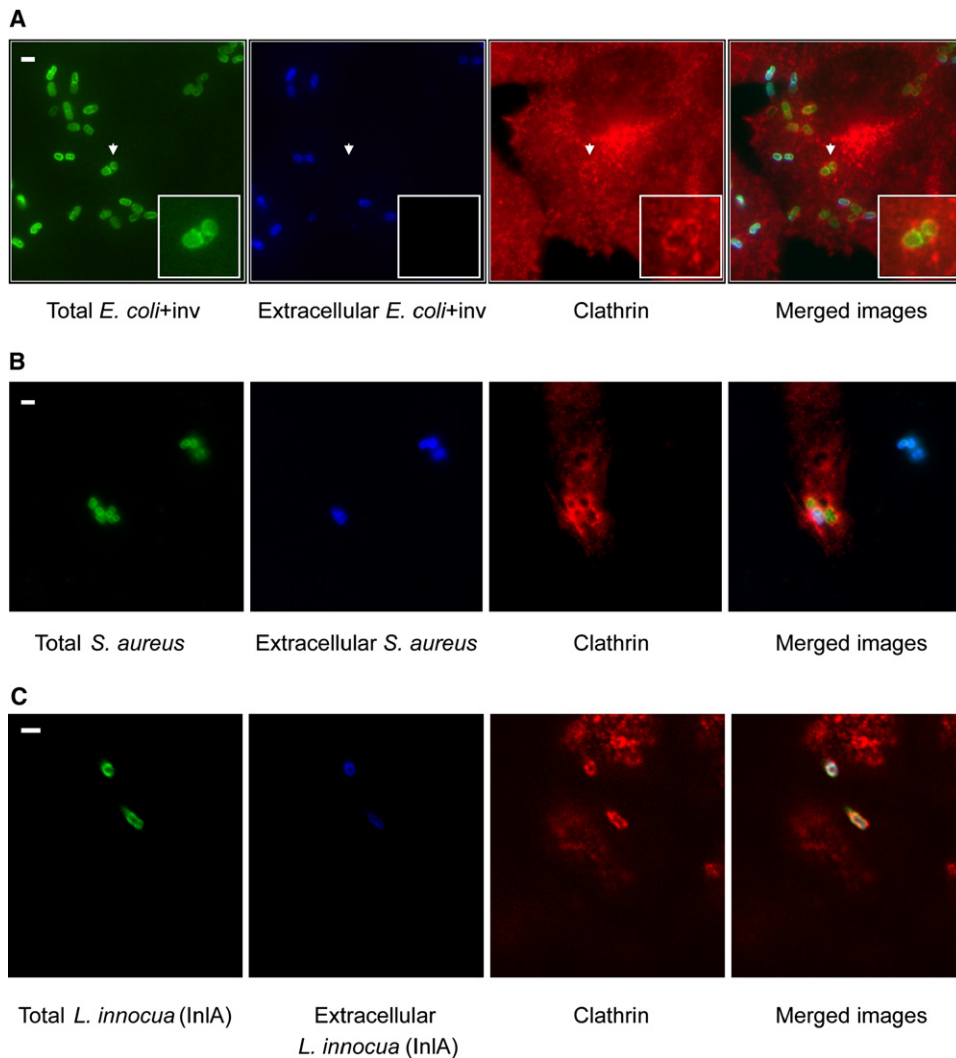
Figure 1. Localization of Endogenous Clathrin during Bacterial Infection
Extracellular bacteria, immunodetected before permeabilization, are shown in blue. Total (extracellular + intracellular) bacteria were detected after permeabilization and are shown in green. Endogenous clathrin was detected using X22 mAb (anticlathrin heavy chain) shown in red. (A) HeLa cells were infected for 10 min with *E. coli* (inv). Areas indicated by the arrows are magnified to better show clathrin surrounding the bacteria. (B) HeLa cells were infected for 20 min with *S. aureus* coated with fibronectin. (C) JEG3 cells were infected for 20 min with *L. innocua* (inlA). Scale bars, 2 μm.

receptor binding protein 2 (Grb2) is an adaptor protein that can direct Cbl to activated receptors and is involved, in some conditions, in cargo entry into clathrin coated pits (Huang and Sorkin, 2005; Jiang et al., 2003; Stang et al., 2004). However, no role for Cbl has been found in the internalization of E-cadherin (Fujita et al., 2002). We thus examined the effect of knocking down the expression of Cbl and Grb2 by siRNA on *E. coli* (inv) and *S. aureus* entry. As shown in Figure 2A, cells with reduced levels of Cbl or Grb2 (Figure 2B) were infected much less efficiently by both *E. coli* (inv) and *S. aureus*. The data presented here, together with our previous data on *Listeria* entering by the InlB/Met pathway (Veiga and Cossart, 2005), point to the critical role of proteins associated with the clathrin-dependent endocytic machinery in zippering pathogens internalization.

Real-Time Imaging of Clathrin and Dynamin Recruitment during Internalization of *Listeria*

Typical endocytic coated pits form by continuous assembly of the clathrin coat (Ehrlich et al., 2004). The size of the vesicle harboring invading bacteria far exceeds the maximal dimensions expected for typical clathrin-coated vesicles. Therefore, study of the dynamics of clathrin recruitment associated with *Listeria* invasion could reveal if a similar or different mechanism of invagination is used. We analyzed, by time-lapse spinning disk confocal microscopy, the entry of GFP-tagged *Listeria* in HeLa cells expressing fluorescent rat clathrin light chain (tdTomato-LCa) (Ehrlich et al., 2004). These cells do not express E-cadherin, and therefore *Listeria* can only enter by using the InlB-Met dependent pathway. We observed a burst of clathrin accumulation surrounding the bacteria as they
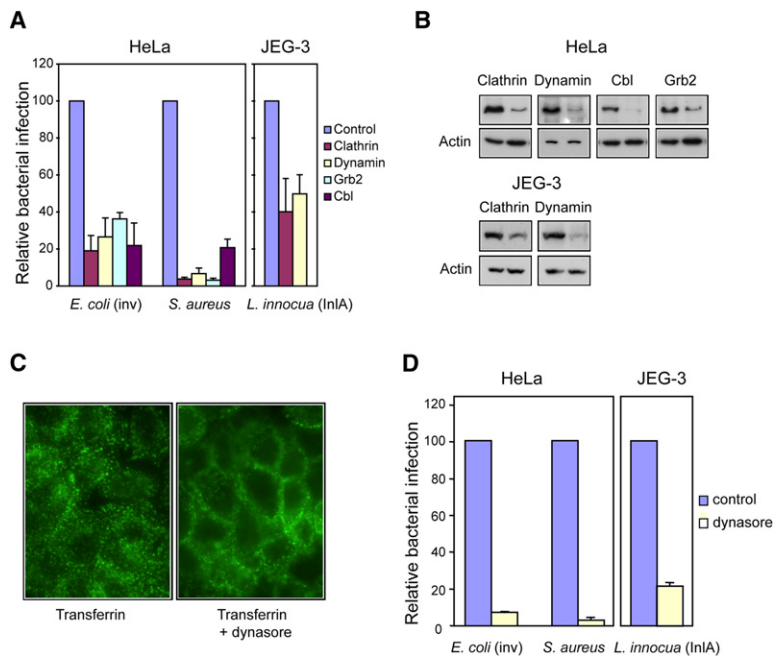
Figure 2. Role of Endocytic Machinery in Bacterial Entry

(A) HeLa and JEG3 cells KD by siRNA for the indicated proteins were infected with *E. coli* (inv), *S. aureus*, or *L. innocua* (inlA). Bacterial infection was measured by CFU (colony-forming unit) counts following gentamicin treatment. Cfu counts obtained from siRNA pretreated cells were normalized to control siRNA (RNA not targeting any cellular mRNA)-treated cells.

(B) Protein KD by siRNA was tested by western-blot. In all cases, the left lane corresponds to the control cells and the right lane corresponds to the cells treated with siRNA against the indicated protein. Actin is shown as a loading control.

(C) Cells were treated or not for 10 min with dynasore (80 μM) and then incubated with FITC-tagged transferrin (25 μg/ml) for 5 min, and transferrin was detected by fluorescence microscopy.

(D) HeLa and JEG3 cells were treated or not (control) with 80 μM dynasore (added 10 min before infection) and infected with the indicated bacteria. Bacterial infection was measured by CFU count after gentamicin assay. CFUs observed from dynasore treated cells were normalized to control (untreated) cells. Error bars represent the standard deviation of at least 4 independent experiments.

entered the cell. This was then followed by clathrin release into the cytosol as bacteria enter (Movie S1 and Figure 3A). Clathrin was not evenly distributed around the bacteria, but instead varied in amounts around the bacteria as they entered the cells, in contrast to the continuous accumulation of clathrin observed during the typical mode of coated pit formation (Boucrot et al., 2006; Ehrlich et al., 2004; Massol et al., 2006). The same clathrin behavior was detected by time lapse wide-field illumination (Movies S2, S3, and S4). The elapsed time of clathrin recruitment around entering bacteria varied from 4 to 12 min (Figure 3B; Figures S2A–S2C), significantly longer than the 40–180 s required for endocytosis of smaller ligands such as for LDL, transferrin, or reovirus (Ehrlich et al., 2004). In addition, we monitored the recruitment of dynamin2-mRFP (Massol et al., 2006) to entering GFP-tagged bacteria (Movie S5 and Figure S2 D). Dynamin 2-mRFP, as shown, was also extensively recruited around bacteria during their internalization and not limited to late time points. AP-2 (the major clathrin adaptor at the plasma membrane) and AP-3 (a putative endosomal clathrin adaptor) were not detected around bacteria during infection (data not shown). We have recently shown using siRNA an unambiguous role for AP-1, a clathrin adaptor involved in the trafficking between endosomes and the trans-Golgi network during *Listeria* invasion (Pizarro-Cerda et al., 2007). However, in the present study as we previously reported, no significant recruitment of AP-1 to entering bacteria was detected although AP-1 containing vesicles were observed near the bacterial invasion area during infection (Movie S6).

Real-Time Imaging of Clathrin Recruitment during Internalization of InlB-Coated Beads

To further study the recruitment of clathrin and clathrin-associated molecules to activated Met in the absence of any other bacterial factor, we used InlB-coated beads whose entry mimics *Listeria* internalization via Met (Braun et al., 1998; Pizarro-Cerda et al., 2002). InlB-coated beads of 1 μm diameter were incubated with different cells expressing fluorescently-tagged (EGFP or tdTomato) clathrin LCa (Ehrlich et al., 2004). The presence of beads absorbed to the top surface of cells was detected by phase contrast microscopy, and the area surrounding specific beads was then monitored using spinning disk time-lapse confocal microscopy. As described for bacterial entry, we also detected a discontinuous and irregular recruitment of clathrin to the beads in contact with the membrane (Movies S7–S9; Figure 3C; Figure S3A). The burst of clathrin associated with the entering beads lasted on average 2–4 min (Figure 3D; Figures S3B and S3C). The duration of clathrin disassembly varied from bead to bead from less than 15 s (Figure 3D) to more than 1 min (Figures S3B and S3C) following InlB-beads entry as defined by the loss of focus when observed by phase contrast and acquisition of clear movement. In contrast, clathrin disassembly from typical clathrin-coated vesicles is always fast (less than 10 s) regardless of their size (Massol et al., 2006). Auxilin is an Hsc70-binding protein required for clathrin disassembly from coated vesicles (Lee et al., 2006; Massol et al., 2006). Auxilin normally accumulates as a burst immediately after the end of clathrin coat assembly and its recruitment coincides with the onset of clathrin
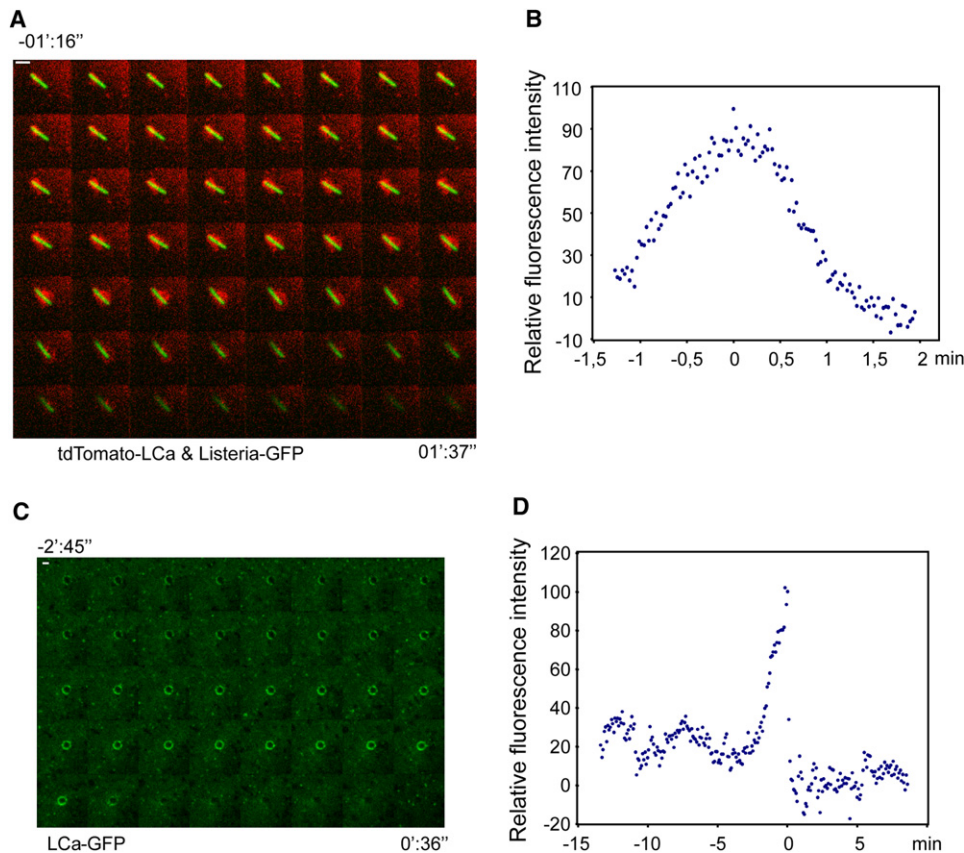
Figure 3. Clathrin Dynamics around Entering Bacteria/Beads

(A) Confocal time series (images acquired every ~1.6 s) from HeLa cells transiently expressing tdTomato-LCa (red) and infected with *Listeria* DH-L1039 expressing GFP (green). The figure shows every other acquisition frame from Movie S1. Scale bar, 2 μm. Bacterial fluorescence decreased during internalization.

(B) Each dot represents the relative fluorescence intensity of tdTomato-LCa surrounding the bacterium at one time point from Movie S1. The maximal fluorescence intensity was arbitrarily considered as 100.

(C) Confocal time series (images acquired every ~5.1 s) from HeLa cells transiently expressing EGFP-LCa (green). The figure shows one every other acquisition frame from Movie S7. Scale bar, 1 μm

(D) Each dot represents the relative fluorescence intensity of EGFP-LCa surrounding the entering bead at a single time point from Movie S7. The maximal fluorescence intensity was arbitrarily considered as 100. Time is shown in minutes (') and seconds ("). Time 0 corresponds to the maximal accumulation of clathrin at the site of entry of bacteria/beads.

disassembly (Massol et al., 2006). As observed in Movie S9, auxilin is also recruited to entering beads, but in sharp contrast to the typical mode of coated vesicle formation, its recruitment parallels the accumulation of clathrin as it associates with InlB-coated beads during their entry (Figure S3C).

In summary, clathrin and molecules belonging to the clathrin-dependent endocytic machinery are recruited to invading bacteria and InlB-coated beads during internalization. The dynamics of their recruitment, however, differs from the behavior observed during the formation of typical coated pits and vesicles during clathrin-mediated endocytosis of smaller cargo.

Entry of Large Ligand-Coated Beads

To further test the hypothesis that a clathrin-based mechanism allows the internalization of large particles, we linked ligands for receptors normally internalized by typical

clathrin coated pits and vesicles to microspheres of the approximate size of a bacterium (1 μm) and assayed them for cellular entry. Beads were coated with fibronectin, the ligand of β1-integrin or with EGF, known to promote endocytosis of its own receptor (EGFR) (Dikic and Giordano, 2003; Johannessen et al., 2006; Stang et al., 2004); these beads accumulate clathrin (Figures 4A and 4B). To examine whether they also internalize, the beads were incubated at 37°C for 2 hours, following a two min centrifugation step with different cell types unable to uptake uncoated microspheres. Figures 4C–4E represent orthogonal views of the confocal plane showing intracellular beads (in green) and actin that delimited the cell contour (in red). Figures 4C and 4D show 1 μm diameter EGF- and fibronectin-coated beads, respectively, already localized inside the cell. 3D reconstruction is available in the Supplemental Data (Movies S10 and S11). Fibronectin-coated beads as large as 5.5 μm in diameter also induced
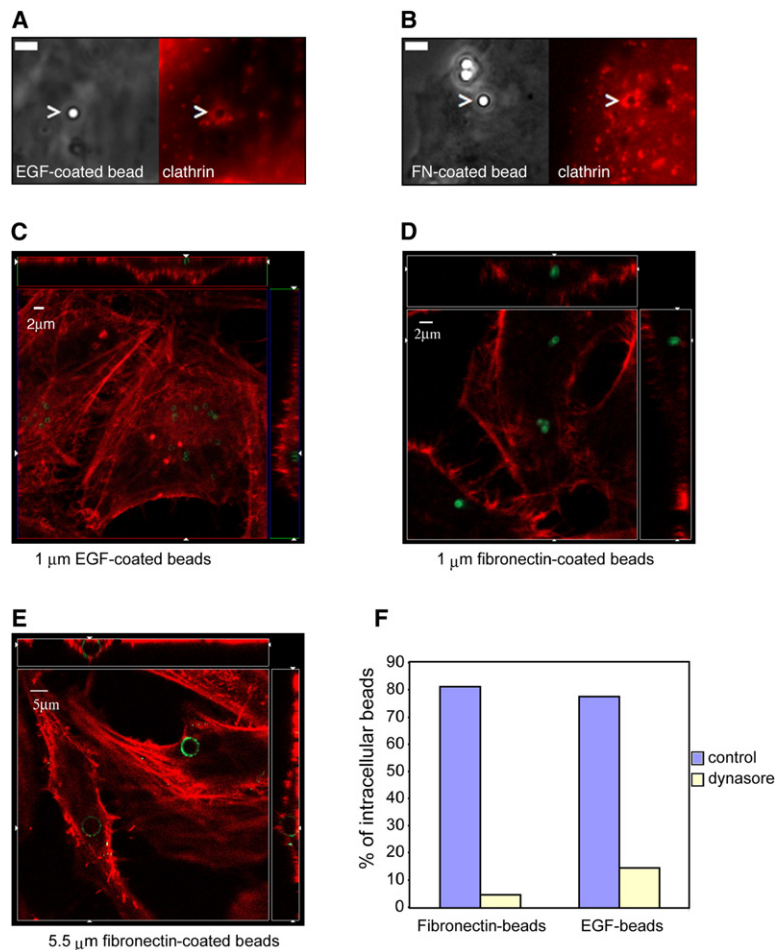
Figure 4. Ligand-Induced Endocytosis of 1 μm Diameter Particles and Larger

Microspheres of 1 or 5.5 μm diameter coated with the indicated proteins were added to HeLa cells. EGF-coated beads (A) or fibronectin (FN)-coated beads (B) were added for 5 min to HeLa cells expressing tdTomato-LCa. Images were acquired at the contact zone of a bead and the cell; phase contrast images show the beads (left panels) and fluorescent images show clathrin (right pannels). Bars, 2 μm. (C, D, and E) Confocal orthogonal views (xy, xz, yz from a single optical section) of intracellular beads (green) and actin (red). The squares represent the xy view corresponding to the z plane indicated by the small arrowheads in the lateral rectangles. The upper and lateral rectangles represent the xz and yz views, respectively. The x and y planes shown correspond to those indicated by the small arrowhead presented in the square. In both, the apical part of the cell looks inward and the lower part, in contact with the slide, to the outside of the figure. (F) Fibronectin or EGF-coated beads were added to HeLa cells treated or not (control) with dynasore. The number of internalized beads is represented with respect to the total beads counted that was taken as 100. A minimum of 300 cells were examined for each condition.

their own internalization (Figure 4E; Movies S12 and S13). These internalization processes are dynamin-dependent since presence of dynasore highly inhibited entry of both types of beads (Figure 4F). Control (serum-coated) beads were unable to enter in the same types of cells (Figure S4).

These data show that ligand-coated particles even larger than an average bacterium can also enter by binding to the appropriate receptor.

The Actin Polymerization Necessary for *Listeria* Entry Follows the Recruitment of Clathrin

A key event in bacterial internalization required to allow wrapping of the plasma membrane around the entering bacteria is the rearrangement of the actin cytoskeleton (Cossart and Sansonetti, 2004). We, therefore, investigated if there exists a connection between clathrin and actin recruitment using as a model *Listeria* entering via the InlB-Met pathway. We first examined the recruitment of clathrin around bacteria and InlB-coated beads at sites of invasion in cells treated with cytochalasin D (a fungal metabolite that inhibits actin polymerization) and compared them to untreated controls. Inhibition of actin rearrangements did not impede the recruitment of clathrin to bacteria or InlB-coated beads (Figures 5A and 5B). In contrast, depletion of clathrin and dynamin by siRNA sig-

nificantly inhibited the recruitment of actin to the bacteria-cell interaction sites (Figures 5C and 5D). These observations demonstrate that clathrin and dynamin recruitment is required for the subsequent actin polymerization needed for *Listeria* entry.

Internalization of Triggering Bacteria Is Clathrin-Independent

To further examine the role of clathrin during bacterial infections, we tested whether clathrin and other proteins involved in clathrin-dependent endocytosis played a role in the internalization of *S. typhimurium* and *S. flexneri*, the paradigms of triggering bacteria. For this purpose, we knocked down by siRNA, clathrin, dynamin, Grb2, and Cbl and analyzed the effects on infection by *S. typhimurium* and *S. flexneri* using gentamicin survival assays. The results of these experiments (performed in parallel to those shown in Figure 2) are presented in Figure 6A; we found that reduction in the levels of clathrin, dynamin, or Grb2 did not affect the infection by *Shigella*. Depletion of Cbl had a minor (15%) reduction in the extent of infection. In the case of *Salmonella*, depletion of clathrin, Grb2, or Cbl did not reduce bacterial entry. KD of clathrin and Grb2 even increased internalization slightly. Interestingly, when the levels of dynamin were reduced, we observed
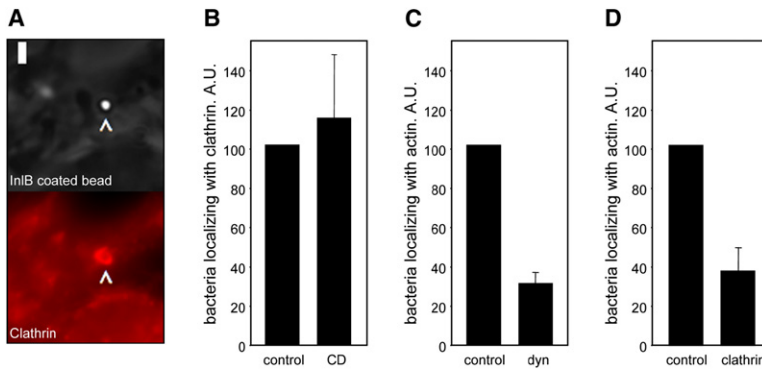
Figure 5. Role of Clathrin in Actin Polymerization around Entering Bacteria

(A) InlB coated beads colocalize with clathrin in the presence of cytochalasin D. Cells were pretreated with cytochalasin D and incubated for 15 min with InlB-coated beads. The figure shows beads imaged by phase contrast (upper panel) and fluorescent images of clathrin (lower panel). Bar, 2 μm. (B) HeLa cells were treated or not (control) with cytochalasin D and incubated with *Listeria* for 5 min. The number of *Listeria* colocalizing with clathrin was then counted. Data are shown as relative values with respect to colocalization in control cells, considered as 100. The experiment was repeat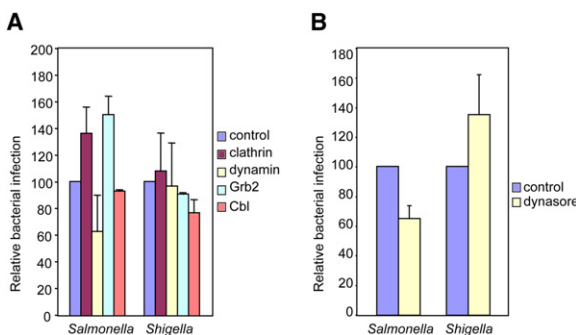ed four times and a minimum of 200 cells were analyzed in each individual experiment. (C and D) HeLa cells were treated with siRNA against dynamin, clathrin, or with control siRNA and incubated with *Listeria* for 5 min. *Listeria* colocalizing with actin was then counted. Data are shown as relative values with respect to control, considered as 100. The experiments were repeated four times and a minimum of 200 cells were analyzed in each experiment. Error bars represent the standard deviation.

a reduction in *Salmonella* internalization of about 35% with respect to control cells. This result agrees with recent observations showing that depending on the cell type, *Salmonella* is also able to partially enter by a type-III secretion system-independent manner, i.e., a zipper-like mechanism (F. Garcia del Portillo, personal communication). Additionally, clathrin was unable to be immunolocalized to *Salmonella* during invasion (data not shown). We then used dynasore to confirm the absence of a major role of dynamin in the entry of triggering bacteria. Treatment with dynasore did not inhibit the internalization of *Shigella* (Figure 6B) and, in agreement with the data using dynamin siRNA, only slightly reduced *Salmonella* infection. Even though clathrin has been reported to localize with *Shigella* foci (Clerc and Sansonetti, 1989), our data collectively confirm that the clathrin-dependent machinery plays no discernable role in the internalization of triggering bacteria. In summary, bacteria injecting their own effectors through a T3SS into the host cells enter independently of a clathrin-

dependent endocytic machinery, in contrast to the process observed for the entry of zippering pathogens.

EPEC Recruits Clathrin to Sites of Bacterial Contact

In order to investigate whether adherent extracellular bacteria that hijack the actin cytoskeleton using a T3SS require clathrin recruitment to sites of bacterial attachment, we used noninvasive EPEC as a model pathogen. During EPEC infections, actin-rich pedestals are generated beneath adherent organisms that remain extracellular (Goosney et al., 2000). These structures protrude from the plasma membrane and, thus, push EPEC away from the host cell. Surprisingly, clathrin localized to the tips of these EPEC pedestals (Figure 7A and Movie S14) and did so in a T3SS-dependent manner (Figure 7B). The recruitment of clathrin was dependent on the translocated intimin receptor (Tir) of EPEC and on the key tyrosine residue (Y474) of Tir that becomes phosphorylated and is required for EPEC pedestal formation (Figure 7C). In cells with reduced levels of clathrin due to treatment with clathrin siRNA (Figure 7E), pedestal formation was abolished, demonstrating that clathrin is required for pedestal generation and highlighting that nonclassical characteristics of clathrin function is exploited during EPEC adherence to host cells (Figure 7D). To test whether actin was required for clathrin localization, we followed the same procedure as that shown in Figure 5B. In cells pretreated with cytochalasin D and subsequently infected with EPEC, clathrin was still recruited to sites of bacterial contact in the absence of actin-filament and pedestal formation (Figure 7F). These studies demonstrate that, as observed for *Listeria*, clathrin associates at bacterial contact sites before, and independently from, actin filaments formation and is required for the subsequent actin polymerization.

DISCUSSION

The data presented here demonstrate that zippering bacteria enter host cells using a form of clathrin- and dynamin-dependent mechanism. Clathrin, dynamin, and auxilin are
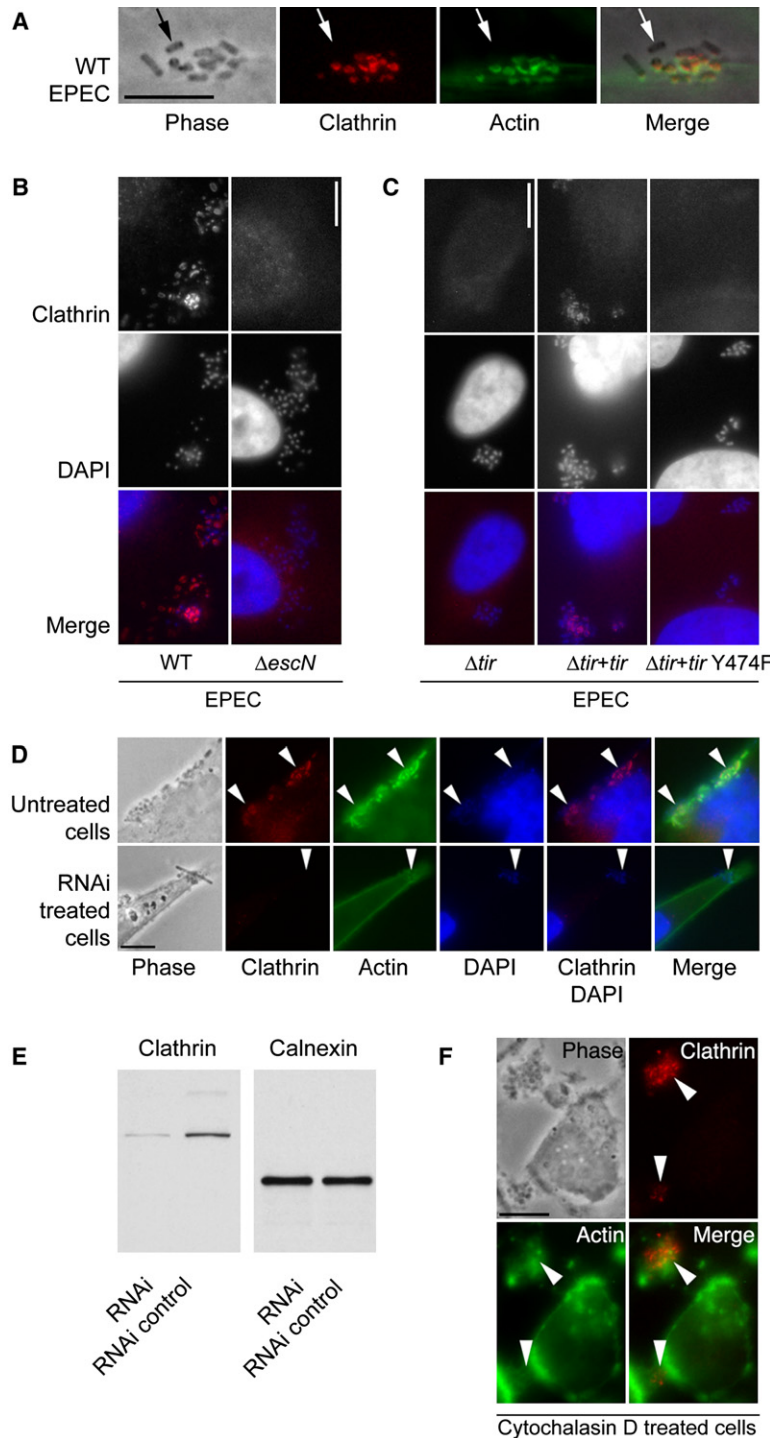

Figure 6. Role of Endocytic Machinery in Entry of Triggering Bacteria

HeLa cells with the indicated proteins KD by siRNA (A) or pretreated with 80 μM dynasore (10 min before infection) (B) were infected with *S. typhimurium* or *S. flexneri*. Bacterial infection was measured by CFU count after gentamicin treatment. CFUs observed from siRNA or dynasore pretreated cells were normalized to controls, i.e., RNAi not targeting any mRNA (A) and untreated cells (B). These experiments were performed in parallel to those shown in Figure 2. Error bars represent the standard deviation of at least 4 independent experiments.

Figure 7. Clathrin Associated with EPEC

(A) Wild-type EPEC infected HeLa cells stained for clathrin and actin. Scale bar, 5 μm. Arrows points to a bacterium that is not attached to the cell. Positive staining is not associated with the nonattached bacterium.

(B) Clathrin immunolocalization on wild-type and ΔescN EPEC infected cells. Clusters of bacteria are visible in the middle row of panels. Scale bar, 10 μm.

(C) Clathrin immunolocalization on Δtir EPEC, Δtir EPEC complemented with EPEC tir (Δtir EPEC + EPEC tir), and Δtir EPEC complemented with tir that has a point mutation at tyrosine 474 (Δtir EPEC + tir Y474F). Clusters of bacteria are visible in the middle row of panels. Scale bar, 10 μm.

(D) Untreated and clathrin RNAi knocked-down cells stained for clathrin, actin, and DAPI. Arrowheads indicate the location of some attached bacteria. Scale bar, 10 μm.

(E) Western blot of clathrin knockdown and control RNAi treated HeLa cells. The blot was immunoreacted with the anti-clathrin antibody used in (A)–(D), then stripped and reprobed with an anti-calnexin antibody to compare the protein loading levels.

(F) Cytochalasin D pretreated HeLa cells infected with EPEC and immunostained for clathrin and actin. Arrowheads indicate the location of some attached bacteria. Scale bar, 10 μm.

recruited to bacteria/beads at the entry sites and inhibition of the classical clathrin-dependent endocytosis system using siRNA against different components of the endocytic machinery or the small molecule inhibitor of dynamin, dynasore, block bacterial entry. Unexpectedly, the variable dynamics of clathrin, dynamin and auxilin recruitment observed by live-cell imaging during entry of bacteria or InlB-coated beads differs from the way by which these proteins are recruited during the process of classical clathrin-dependent endocytosis during internalization of smaller ligands. Beads coated with fibronectin or EGF were also internalized in a dynamin-dependent manner, supporting the hypothesis that this process is ligand-induced.

How clathrin and its associated proteins are assembled to allow the entry of large vesicles remains unknown. The fluorescence microscopy data presented here, although clearly showing the presence of clathrin around entering bacteria and beads, lack the spatial resolution required to precisely address this important question. To examine this, it will be necessary to perform electron tomography studies.

Although clathrin is responsible for the internalization of several zippering bacteria, it is also possible that other types of clathrin-independent endocytic machineries could also be involved. Viruses are able to enter by several types of endocytosis (Marsh and Helenius, 2006), and one could anticipate a similar diversity for bacteria. Previously, it has been shown that clathrin is mobilized during *S. flexneri* infections in Hep2 cells (Clerc and Sansonetti, 1989). Nevertheless, our study was unable to detect a functional involvement for the clathrin-dependent endocytic machinery for the entry of triggering bacteria.

Another unexpected observation was the recruitment of clathrin at the bacterial contact sites during EPEC infections and its essential role in this process. Like with the zippering bacteria, clathrin (shown here) and dynamin recruitment (Unsworth et al., 2007) are also ligand (Tir)-dependent, but contrary to what is observed during infections of intracellular zippering bacteria, it does not lead to bacterial internalization. It remains unclear why the bacterial receptor Tir does not induce endocytosis, in contrast to other receptors that do so such as EGF-R, Integrins, Met, and E-cadherin. EPEC is known to be antiphagocytic (Celli et al., 2001), and exploitation of the clathrin pathway may contribute to this virulence attribute. As clathrin is required for the generation of EPEC pedestals, the interactions of clathrin with other pedestal components will likely be a key factor in identifying how this protein functions at this site.

The entry of zippering invasive bacteria has been extensively studied during the last two decades, and the rearrangement of the actin cytoskeleton has been considered a key event in this process (Cossart and Sansonetti, 2004). Activated by bacterial ligands, cellular receptors were shown to trigger signaling cascades that recruit and activate the Arp2/3 complex, thereby promoting the actin polymerization at the bacterial entry site. Actin polymerization allows the cellular membrane to remodel and engulf the entering bacteria. Inhibiting actin rearrangements using the fungal metabolite cytochalasin D or other strategies such as depletion of dynamin, cortactin, or CD2AP by siRNA prevent bacterial internalization (Cossart and Sansonetti, 2004; Veiga and Cossart, 2005). In an effort to understand the whole process of bacterial internalization, we studied the relationship between actin polymerization and clathrin recruitment during bacterial invasion. The fact that treatment with cytochalasin D did not affect the recruitment of clathrin to the *Listeria*-cell contact sites together with the observation that cellular depletion of clathrin and dynamin impaired the actin polymerization around bacteria reveals that accumulation of clathrin and dynamin are necessary events that occur upstream

of the waves of actin polymerization allowing *Listeria* using the InlB/Met pathway to enter. This is similar to the situation during EPEC infections, where clathrin recruitment seems to be independent and taking place before actin filament polymerization at bacterial/host cell contact points. Other studies in mammalian cells show a limited degree of association between clathrin and actin recruitment during the endocytosis of small ligands such as transferrin (Perrais and Merrifield, 2005; Yarar et al., 2007). The exact connection between the clathrin and actin-based machineries remains to be determined. Possible links between the two events are the interactions between dynamin and cortactin, which itself can activate the Arp2/3 complex. An important role may also be played by CD2AP, a protein that links cortactin with Cbl and the endocytic machinery (Lynch et al., 2003).

Future studies are required to elucidate the structure of the clathrin coat surrounding the entering bacteria and to better define the link between the actin and clathrin systems during bacterial entry, pedestal formation, and potentially other virulence strategies.

EXPERIMENTAL PROCEDURES

Cells, Bacteria, and Growth Conditions

The cell lines used were HeLa (ATCC number CCL-2), Caco-2 (ATCC number HTB-37), JEG-3 (ATCC number HTB-36), MDCK (ATCC number CCL-34), BSC-1 (ATCC number CCL-26) stably expressing EGFP-LCa (Ehrlich et al., 2004), U-373 mg astrocytes (ATCC number HTB-17), MDCK (ATCC number CRL-2285), and murine fibroblast. They were grown as recommended by ATCC. The bacterial strains used were *L. monocytogenes* EGD BUG 600, EGDΔinlB (pAT18pprot+LRRs-IR inlB-SPA BUG 1641; Bierne et al., 2001); BUG 2378 (BUG1641 expressing GFP, this work); DH-L1039 (gift from Darren Higgins; Shen and Higgins, 2005); *L. innocua* (inlA) BUG 1489 (Gaillard et al., 1991); *S. aureus* ISP479r and V329 (gifts from Iñigo Lasa); *E. coli* (inv) (gift from Guy van Tran Nhieu); *Salmonella enterica* serovar *Typhimurium* SL1344 (gift from Francisco Garcia del Portillo); and *Shigella flexneri* M90T (gift from Philippe Sansonetti). Enteropathogenic *E.coli* (EPEC) strains included wild-type EPEC strain E2348/69 as well as ΔescN mutant from the same strain, wild-type EPEC strain JPN15 and mutant strains in that background that included Δtir, Δtir complemented with EPEC *tir*, and Δtir mutant complemented with EPEC *tir* Y474F (DeVinney et al., 2001).

The mediums used for bacterial growth were BHI for *Listeria* and *Staphylococcus* strains, LB for *E. coli* (inv), *Salmonella* and EPEC, and BTCS for *Shigella*. When necessary, 5 μg/ml of erythromycin, 7 μg/ml of chloramphenicol, or 100 μg/ml of ampicillin were added. BUG 2378 was constructed by electroporation of nonreplicative plasmid pPL3 s-gfp (Shen and Higgins, 2005) on BUG 1641.

Plasmids

pPL3 s-gfp was a gift from Prof. Darren Higgins (Shen and Higgins, 2005), Plasmid encoding dynamin2-GFP was a gift from Prof. Mark A. McNiven (Cao et al., 1998). Plasmid encoding EGFP-LCa, tdTomato-LCa, EGFP-aux1 and dynamin2-mRFP were described elsewhere (Ehrlich et al., 2004; Massol et al., 2006). pσ1-tdTomato codifies for the σ1 subunit of AP-1 fused to td-Tomato. Plasmids containing EPEC *tir* and EPEC *tir* Y474F are described elsewere (DeVinney et al., 2001).

Antibodies and Reagents

The antibodies and reagents used in this study were Alexa Fluor 546-conjugated phalloidin, Alexa Fluor 488-, 546-, and 647-conjugated

goat anti-rabbit and goat anti-mouse antibodies (Molecular Probes). Mouse monoclonal (mAb) anti-β-actin (AC15; Sigma), anti-Cbl (BD pharmingen), mAb X22 anti-clathrin heavy-chain, mAb anti-clathrin heavy-chain (BD pharmingen), rabbit polyclonal antibody (pAb), anti-dynamin2 (Calbiochem), mAb anti-E-cadherin, pAb anti-*E. coli* (Biodesign), pAb (Z-12) anti-EGF (Santa Cruz), pAb (H-896) anti-eps15 (Santa Cruz), pAb anti-fibronectin (Sigma), pAb (C-23) anti-Grb2 (Santa Cruz), rabbit serum anti-*Listeria* (R11), pAb anti-*S. aureus* (Biogenesis), cytochalasin D (Sigma), fluorescein-conjugated transferrin (Invitrogen-Molecular Probes). Dynasore (Macia et al., 2006) (80 μM in 0.4% DMSO final) was directly dissolved in the cellular growth medium (typically D-MEM or MEM; GIBCO with or without 1% Nu-Serum [BD Biosciences] without significant differences).

Ligand-Coating Beads
Typically, 1 mg of streptavidin-coated microspheres of 0.93 or 5.47 μm diameter (Bangs labs) were bound to 400 μg of the following biotinylated proteins: recombinant human E-cadherin/FC chimera (R&D systems), recombinant human EGF (Sigma) and (R&D systems), fibronectin from human plasma (Sigma).

Protein Biotinylation
The proteins described above resuspended in PBS were bound to biotinamidohexanoic acid NHS ester (Sigma) for 2 hr at 22°C and then passed through a sephadex G25 column (GE Healthcare). When needed, samples containing biotinylated proteins were concentrated by using centrifugal filter devices (Amicon Ultra, Millipore). InlB was bound to carboxylated microspheres of 1.04 μm diameter (Bangs labs) as described (Braun et al., 1998).

RNAi Assays
Double-stranded RNA against Cbl sense (s) 5′-GGG AAA AGA AAG AAU GUA Utt-3′, antisense (as) 5′-AUA CAU UCU UUC UUU UCC Ctc-3′; Clathrin heavy-chain s 5′-GGC CCA GGU GGU AAU CAU Utt-3′, as 5′-AAU GAU UAC CAC CUG GGC Ctg-3′; or On-Target SMART pool against clathrin heavy chain (Dharmacon), Grb2 s 5′-GGU UUU GAA CGA AGA AUG Utt-3′, as 5′-ACA UUC UUC GUU CAA AAC Ctt-3′, eps15 s 5′-GGU UGA UAC AGG CAA UAC Utt-3′, as 5′-AGU AUU GCC UGU AUC AAC Ctg-3′, Dynamin II s 5′ GGA GAU UGA AGC AGA GAC Ctt-3′, as 5′-GGU CUC UGC UUC AAU CUC Ctg-3′ were purchased from Ambion and Eurogentec. Control RNA (Silencer Negative Control 1 siRNA) was purchased from Ambion and siCONTROL nontargeting siRNA pool was purchased from Dharmacon. Transfections were performed using oligofectamine (Invitrogen) for HeLa cells and Dharmafect1 (Dharmacon) for JEG3 cells. They were used as recommended by the manufacturers. Cells were tested 48 or 72 hr after transfections.

Differential Immunofluorescence Labeling
Differential immunofluorescence labeling was performed as previously described (Pizarro-Cerda and Cossart, 2006b). Briefly, extracellular bacteria or beads were stained using specific antibodies before permeabilization. Second staining was performed after cellular permeabilization. Using secondary antibodies with two different fluorochromes before and after permeabilization allows discrimination between adherent extracellular bacteria/beads and those that have been internalized. As HeLa cells produced low amounts of fibronectin, *S. aureus* was incubated with purified fibronectin before cellular challenging in order to facilitate its entry.

Gentamicin Survival Assays
Gentamicin survival assays were performed as previously described (Pizarro-Cerda and Cossart, 2006b). Briefly, after 1 hour of bacterial challenge, gentamicin was added to the culture medium (20–40 μg/ml depending of the bacteria) for two hours. The antibiotic gentamicin is very poorly internalized in mammalian cells, killing only the extracellular bacteria being the intracellular bacteria protected from the genta-

micin. Bacterial internalization was measured by plating the cell lysates in agar-containing plates and counting bacterial colonies.

Immunolabeling and Wide-Field Microscopy
For immunolabeling, cells were fixed with a PFA solution (3% in PBS) for 15–30 min, then permeabilized (0.1% Triton X-100 for 5 min in PBS). Antibodies were incubated for 30 min at RT or overnight at 4°C in blocking solution. Images were acquired on a fluorescence inverted microscope (Axiovert 135; Carl Zeiss MicroImaging, Inc.) equipped with a cooled charge-coupled device camera (MicroMax 5 MHz; Princetown Instruments) driven by Metamorph Imaging System software (Universal Imaging Corp). EPEC images were acquired using a Zeiss Axiophot microscope.

Time-Lapse Wide-Field Microscopy
Images were acquired with a motorized inverted fluorescence microscope (Axiovert 200I, Carl Zeiss MicroImaging) equipped with a temperature-controlled stage using 100× lenses (Carl Zeiss, Inc). Fluorescent illumination was driven by an ultra-high-speed wavelength switcher Lambda DG4 (Sutter Instrument) equipped with a 175 W xenon arc lamp and excitation filters for GFP (Excitation = 480; Emission = 525) and DsRed (Excitation = 565; Emission = 620) (Chroma Technology). Emission filters were selected using a high-speed Lambda 10 filter wheel (Sutter Instrument). Images were acquired with exposure times between 100 and 500 ms with a cooled, digital, charge-coupled device camera (CoolSNAPHQ, Photometrics). All devices were controlled by MetaMorph Imaging System software (Universal Imaging).

Confocal Images from Live Samples
Confocal images from live samples were acquired with a spinning disk confocal head (Perkin Elmer Co., Boston, MA) coupled to a fully motorized epifluorescence microscope (Axiovert 200M; Carl Zeiss, Inc.; Thornwood, NY) using 100× lenses (Carl Zeiss, Inc.) under control of SlideBook 4 (Intelligent Imaging Innovations, Denver, CO). Digital images were obtained with a cool CCD camera (CoolSnapHQ, Photometrics) with 2 × 2 binning and spatial resolution of 0.13 μm/pixel. Images were acquired with exposure times between 100 and 500 ms from cells maintained at 37°C using a heated stage (20/20 Technology, Inc.). A krypton-argon laser (Mellets Griot) emitting at 488 and 568 nm was used to excite EGFP and tdTomato. Images were analyzed using SlideBook 4 (Intelligent Imaging Innovations) and ImageJ (http://rsb.info.nih.gov/ij/). Internalization of bacteria and beads was followed on cells in which dynamics of clathrin and dymamin recruitment to classical vesicles behave as previously described (Boucrot et al., 2006; Ehrlich et al., 2004; Massol et al., 2006).

Confocal Images from Fixed Samples
Confocal images from fixed samples were acquired using a laser scanning confocal microscope (Zeiss LSM510) using 100× lenses (Carl Zeiss, Inc.) under control of LSM (Carl Zeiss, Inc.). Argon and neon-helio lasers (Mellets Griot) emitting at 488, 543, and 633 nm were used. Confocal slice images (0.17 μm) were acquired. The images were treated using Osirix (http://www.osirix-viewer.com/), ImageJ, and LSM (Carl Zeiss, Inc).

Supplemental Data
The Supplemental Data include four supplemental figures and 15 supplemental movies and can be found with this article online at http://www.cellhostandmicrobe.com/cgi/content/full/2/5/340/DC1/.

REFERENCES

Agerer, F., Lux, S., Michel, A., Rohde, M., Ohlsen, K., and Hauck, C.R. (2005). Cellular invasion by *Staphylococcus aureus* reveals a functional link between focal adhesion kinase and cortactin in integrin-mediated internalisation. J. Cell Sci. *118*, 2189–2200.

Aggeler, J., and Werb, Z. (1982). Initial events during phagocytosis by macrophages viewed from outside and inside the cell: Membrane-particle interactions and clathrin. J. Cell Biol. *94*, 613–623.

Bierne, H., Gouin, E., Roux, P., Caroni, P., Yin, H.L., and Cossart, P. (2001). A role for cofilin and LIM kinase in *Listeria*-induced phagocytosis. J. Cell Biol. *155*, 101–112.

Boucrot, E., Saffarian, S., Massol, R., Kirchhausen, T., and Ehrlich, M. (2006). Role of lipids and actin in the formation of clathrin-coated pits. Exp. Cell Res. *312*, 4036–4048.

Braun, L., Ohayon, H., and Cossart, P. (1998). The InlB protein of *Listeria* monocytogenes is sufficient to promote entry into mammalian cells. Mol. Microbiol. *27*, 1077–1087.

Cao, H., Garcia, F., and McNiven, M.A. (1998). Differential distribution of dynamin isoforms in mammalian cells. Mol. Biol. Cell *9*, 2595–2609.

Celli, J., Olivier, M., and Finlay, B.B. (2001). Enteropathogenic *Escherichia coli* mediates antiphagocytosis through the inhibition of PI 3-kinase-dependent pathways. EMBO J. *20*, 1245–1258.

Cheng, Y., Boll, W., Kirchhausen, T., Harrison, S.C., and Walz, T. (2007). Cryo-electron tomography of clathrin-coated vesicles: Structural implications for coat assembly. J. Mol. Biol. *365*, 892–899.

Clerc, P.L., and Sansonetti, P.J. (1989). Evidence for clathrin mobilization during directed phagocytosis of *Shigella flexneri* by HEp2 cells. Microb. Pathog. *7*, 329–336.

Conner, S.D., and Schmid, S.L. (2003). Regulated portals of entry into the cell. Nature *422*, 37–44.

Cossart, P., and Sansonetti, P.J. (2004). Bacterial invasion: The paradigms of enteroinvasive pathogens. Science *304*, 242–248.

DeVinney, R., Puente, J.L., Gauthier, A., Goosney, D., and Finlay, B.B. (2001). Enterohaemorrhagic and enteropathogenic Escherichia coli use a different Tir-based mechanism for pedestal formation. Mol. Microbiol. *41*, 1445–1458.

Dikic, I., and Giordano, S. (2003). Negative receptor signalling. Curr. Opin. Cell Biol. *15*, 128–135.

Dikic, I., Szymkiewicz, I., and Soubeyran, P. (2003). Cbl signaling networks in the regulation of cell function. Cell. Mol. Life Sci. *60*, 1805–1827.

Ehrlich, M., Boll, W., Van Oijen, A., Hariharan, R., Chandran, K., Nibert, M.L., and Kirchhausen, T. (2004). Endocytosis by random initiation and stabilization of clathrin-coated pits. Cell *118*, 591–605.

Fujita, Y., Krause, G., Scheffner, M., Zechner, D., Leddy, H.E., Behrens, J., Sommer, T., and Birchmeier, W. (2002). Hakai, a c-Cbl-like protein, ubiquitinates and induces endocytosis of the E-cadherin complex. Nat. Cell Biol. *4*, 222–231.

Gaillard, J.L., Berche, P., Frehel, C., Gouin, E., and Cossart, P. (1991). Entry of *L. monocytogenes* into cells is mediated by internalin, a repeat protein reminiscent of surface antigens from gram-positive cocci. Cell *65*, 1127–1141.

Goosney, D.L., Gruenheid, S., and Finlay, B.B. (2000). Gut feelings: Enteropathogenic *E. coli* (EPEC) interactions with the host. Annu. Rev. Cell Dev. Biol. *16*, 173–189.

Grundmeier, M., Hussain, M., Becker, P., Heilmann, C., Peters, G., and Sinha, B. (2004). Truncation of fibronectin-binding proteins in *Staphylococcus aureus* strain Newman leads to deficient adherence and host cell invasion due to loss of the cell wall anchor function. Infect. Immun. *72*, 7155–7163.

Heuser, J. (1989). Effects of cytoplasmic acidification on clathrin lattice morphology. J. Cell Biol. *108*, 401–411.

Hinshaw, J.E. (2000). Dynamin and its role in membrane fission. Annu. Rev. Cell Dev. Biol. *16*, 483–519.

Huang, F., and Sorkin, A. (2005). Grb2-mediated recruitment of the ring domain of Cbl to the EGF receptor is essential and sufficient to support receptor endocytosis. Mol Biol Cell. *16*, 1268–1281.

Isberg, R.R., and Falkow, S. (1985). A single genetic locus encoded by *Yersinia pseudotuberculosis* permits invasion of cultured animal cells by Escherichia coli K-12. Nature *317*, 262–264.

Isberg, R.R., and Leong, J.M. (1990). Multiple beta 1 chain integrins are receptors for invasin, a protein that promotes bacterial penetration into mammalian cells. Cell *60*, 861–871.

Jiang, X., Huang, F., Marusyk, A., and Sorkin, A. (2003). Grb2 regulates internalization of EGF receptors through clathrin-coated pits. Mol. Biol. Cell *14*, 858–870.

Johannessen, L.E., Pedersen, N.M., Pedersen, K.W., Madshus, I.H., and Stang, E. (2006). Activation of the epidermal growth factor (EGF) receptor induces formation of EGF receptor- and Grb2-containing clathrin-coated pits. Mol. Cell. Biol. *26*, 389–401.

Kaabeche, K., Guenou, H., Bouvard, D., Didelot, N., Listrat, A., and Marie, P.J. (2005). Cbl-mediated ubiquitination of alpha5 integrin subunit mediates fibronectin-dependent osteoblast detachment and apoptosis induced by FGFR2 activation. J. Cell Sci. *118*, 1223–1232.

Kirchhausen, T. (2000). Three ways to make a vesicle. Nat. Rev. Mol. Cell Biol. *1*, 187–198.

Lecuit, M., Dramsi, S., Gottardi, C., Fedor-Chaiken, M., Gumbiner, B., and Cossart, P. (1999). A single amino acid in E-cadherin responsible for host specificity towards the human pathogen *Listeria monocytogenes*. EMBO J. *18*, 3956–3963.

Lee, D.W., Wu, X., Eisenberg, E., and Greene, L.E. (2006). Recruitment dynamics of GAK and auxilin to clathrin-coated pits during endocytosis. J. Cell Sci. *119*, 3502–3512.

Lynch, D.K., Winata, S.C., Lyons, R.J., Hughes, W.E., Lehrbach, G.M., Wasinger, V., Corthals, G., Cordwell, S., and Daly, R.J. (2003). A Cortactin-CD2-associated protein (CD2AP) complex provides a novel link between epidermal growth factor receptor endocytosis and the actin cytoskeleton. J. Biol. Chem. *278*, 21805–21813.

Macia, E., Ehrlich, M., Massol, R., Boucrot, E., Brunner, C., and Kirchhausen, T. (2006). Dynasore, a cell-permeable inhibitor of dynamin. Dev. Cell *10*, 839–850.

Marsh, M., and Helenius, A. (2006). Virus entry: Open sesame. Cell *124*, 729–740.

Massol, R.H., Boll, W., Griffin, A.M., and Kirchhausen, T. (2006). A burst of auxilin recruitment determines the onset of clathrin-coated vesicle uncoating. Proc. Natl. Acad. Sci. USA *103*, 10265–10270.

Matlin, K.S., Reggio, H., Helenius, A., and Simons, K. (1981). Infectious entry pathway of influenza virus in a canine kidney cell line. J. Cell Biol. *91*, 601–613.

McMahon, H.T. (1999). Endocytosis: An assembly protein for clathrin cages. Curr. Biol. *9*, R332–R335.

McNiven, M.A., and Thompson, H.M. (2006). Vesicle formation at the plasma membrane and trans-Golgi network: The same but different. Science *313*, 1591–1594.

Merrifield, C.J., Perrais, D., and Zenisek, D. (2005). Coupling between clathrin-coated-pit invagination, cortactin recruitment, and membrane scission observed in live cells. Cell *121*, 593–606.

Orth, J.D., and McNiven, M.A. (2003). Dynamin at the actin-membrane interface. Curr. Opin. Cell Biol. *15*, 31–39.

Parker, J.S., and Parrish, C.R. (2000). Cellular uptake and infection by canine parvovirus involves rapid dynamin-regulated clathrin-mediated endocytosis, followed by slower intracellular trafficking. J. Virol. *74*, 1919–1930.

Perrais, D., and Merrifield, C.J. (2005). Dynamics of endocytic vesicle creation. Dev. Cell *9*, 581–592.

Petrelli, A., Gilestro, G.F., Lanzardo, S., Comoglio, P.M., Migone, N., and Giordano, S. (2002). The endophilin-CIN85-Cbl complex mediates ligand-dependent downregulation of c-Met. Nature *416*, 187–190.

Pizarro-Cerda, J., and Cossart, P. (2006a). Bacterial adhesion and entry into host cells. Cell *124*, 715–727.

Pizarro-Cerda, J., and Cossart, P. (2006b). *Listeria monocytogenes*: Techniques to analyze bacterial infection in vitro. In Cell Biology: A Laboratory Handbook, J.E. Celis, N. Carter, K. Simons, J.V. Small, T. Hunter, and D. Shotton, eds. (London: Academic Press), pp. 407–415.

Pizarro-Cerda, J., Jonquieres, R., Gouin, E., Vandekerckhove, J., Garin, J., and Cossart, P. (2002). Distinct protein patterns associated with *Listeria monocytogenes* InlA- or InlB-phagosomes. Cell. Microbiol. *4*, 101–115.

Pizarro-Cerda, J., Payrastre, B., Wang, Y.J., Veiga, E., Yin, H.L., and Cossart, P. (2007). Type II phosphatidylinositol 4-kinases promote *Listeria monocytogenes* entry into target cells. Cell. Microbiol. *10*, 1167–1175. 10.1111/j.1462–5822.2007.00967.x.

Raiborg, C., Wesche, J., Malerod, L., and Stenmark, H. (2006). Flat clathrin coats on endosomes mediate degradative protein sorting by scaffolding Hrs in dynamic microdomains. J. Cell Sci. *119*, 2414–2424.

Shen, A., and Higgins, D.E. (2005). The 5′ untranslated region-mediated enhancement of intracellular listeriolysin O production is required for *Listeria monocytogenes* pathogenicity. Mol. Microbiol. *57*, 1460–1473.

Shen, Y., Naujokas, M., Park, M., and Ireton, K. (2000). InlB-dependent internalization of *Listeria* is mediated by the Met receptor tyrosine kinase. Cell *103*, 501–510.

Sorkin, A. (2004). Cargo recognition during clathrin-mediated endocytosis: A team effort. Curr. Opin. Cell Biol. *16*, 392–399.

Stang, E., Blystad, F.D., Kazazic, M., Bertelsen, V., Brodahl, T., Raiborg, C., Stenmark, H., and Madshus, I.H. (2004). Cbl-dependent Ubiquitination Is Required for Progression of EGF Receptors into Clathrin-coated Pits. Mol. Biol. Cell *15*, 3591–3604.

Unsworth, K.E., Mazurkiewicz, P., Senf, F., Zettl, M., McNiven, M., Way, M., and Holden, D.W. (2007). Dynamin is required for F-actin assembly and pedestal formation by enteropathogenic *Escherichia coli* (EPEC). Cell. Microbiol. *9*, 438–449.

Veiga, E., and Cossart, P. (2005). *Listeria* hijacks the clathrin-dependent endocytic machinery to invade mammalian cells. Nat. Cell Biol. *7*, 894–900.

Veiga, E., and Cossart, P. (2006). The role of clathrin-dependent endocytosis in bacterial internalization. Trends Cell Biol. *16*, 499–504.

Yarar, D., Waterman-Storer, C.M., and Schmid, S.L. (2007). SNX9 Couples Actin Assembly to Phosphoinositide Signals and Is Required for Membrane Remodeling during Endocytosis. Dev. Cell *13*, 43–56.